

## CHAPTER 122

# Numerical determination of wave induced flow in rubble mound breakwaters.

Sun ZC<sup>1</sup>, Williams AF<sup>2</sup>, Allsop NWH<sup>2</sup>

### 1 ABSTRACT

This paper describes a numerical model of wave action onto and into a rubble mound breakwater. The model is constructed of two parts, the wave action on the exterior of the mound in which a boundary element method is used and flow inside the rubble mound in which a finite element method is used. The two parts of the model are coupled by demanding continuity of flow through the front face of the breakwater. The predicted pressures within the core of the rubble mound are compared with data collected from physical model tests.

### 2 INTRODUCTION

The problem is that of wave action onto and into a rubble mound breakwater as illustrated in Fig(1). External wave action on the breakwater induces wave action within the porous material of the rubble mound. The stability of both the rubble mound core and the external armour layers is dependent on the pore water pressures within the structure. Our aim is to model the wave motion within the rubble mound, and calculate the instantaneous pore pressures as they change under wave action.

A complete model needs to incorporate all of the following physical processes: Random wave motion external to the breakwater and uprush onto the breakwater face. Energy dissipation caused by wave breaking and friction at the breakwater surface. The transport of water through the front face of the breakwater. The flow of water through the porous material of the breakwater core. Here the flow is non-Darcy or turbulent and the flow rate is unsteady. The effect of entrained air in the flow of water through the porous material. A complete model must also be able to deal with complex breakwater geometries, such as berms and layers of armour and filter

---

<sup>1</sup>Dalian University of Technology, Dalian, China.

<sup>2</sup>Coastal Structures section, Hydraulics Research, Wallingford, OX10 8BA, UK.

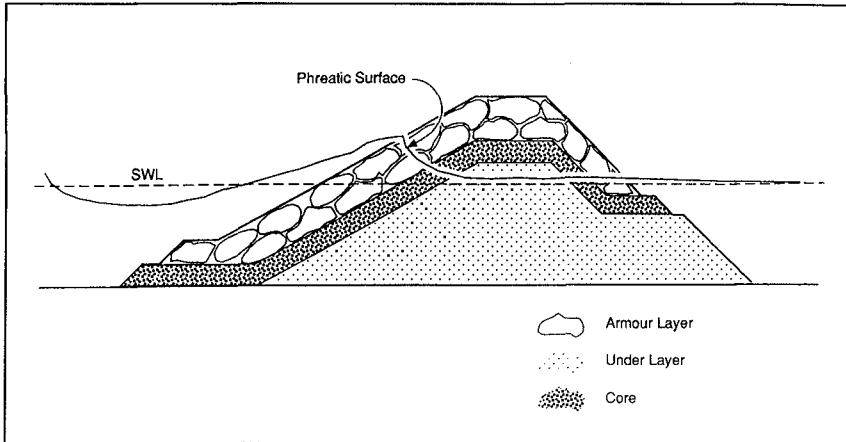


**Figure 1** Wave action on a rubble mound breakwater.

materials.

No model is presently able to incorporate all of these processes. Analytical solutions such as that proposed by Sollitt & Cross (1972) by necessity require the geometry to be simplified to a homogeneous rectangle with vertical faces. Madsen & White (1976) also developed an analytical solution which uses assumptions of rectangular geometry and linear periodic wave theory. They improved the range of application of their model by representing multi-layered trapezoidal breakwaters with a "hydraulically equivalent" homogeneous rectangular structure. Predictions of wave reflection and transmission can be made using analytical models of this type. Unfortunately the simplifying assumptions and averaging processes necessary to arrive at an analytical solution make it impossible to calculate local instantaneous water velocities or pressures.

To find the local instantaneous velocities and pressures required for the investigation of breakwater stability, a method is required that does not make gross assumptions about the structure geometry or involve integration of the solution over a wave period. These requirements may only be met by use of a numerical model. McCorquodale & Nasser (1974), Nasser (1974) and Hannoura (1978) have all developed numerical models for flow with the porous material of the breakwater. A hybrid finite element/difference model is described by Hannoura & McCorquodale (1985), in which the time integration is carried out by a finite difference method and the space integration is solved by use of a finite element method. The model is restricted in its application as it only simulates the flow within the breakwater, and requires the boundary condition on the seaward face of the breakwater to be supplied from empirical data or an alternative numerical model.

A more comprehensive model is at present in development under the European MAST G6-S project (Meer et al. (1992)). This model utilises the

volume of fluid (VOF) technique similar to the SOLA-VOF developed by Nicholas, Hirt & Hotchkiss (1980). VOF methods are the most promising way forward to a complete model which includes the effects of wave runup and breaking. Unfortunately VOF models are computationally intensive and at present a main frame computing facilities are required for implementation. The model being developed under MAST still requires further work and it may be several years before a fully working VOF model is available.

At Wallingford we have developed an intermediate numerical model which divides the problem into two parts:- a). The external wave action which produces pressures on the outer surface of the breakwater. (The external flow field). b). The internal flow within the breakwater driven by the pressures induced by the external flow field. (The internal flow field). The internal flow field (b) is modelled by the use of a finite element method. The external flow field (a) is calculated by use of a boundary element method. These two models are then coupled by allowing water to flow through the shared boundary. The ability to model the wave action on the exterior face of the breakwater means that support from physical model tests, as is necessary for the implementation of the Hannoura & McCorquodale (1985) model, is not required.

### 3. THE EXTERNAL FLOW FIELD

Here the wave motion is calculated in two dimensions by use of a boundary element method. The program used is a variation of the program developed by Shih (1989), from the method described by Vinje & Brevig (1981).

#### 3.1 GENERAL PRINCIPLES

The fluid is assumed to be both incompressible and irrotational. Such a two dimensional flow field can be described by either one of the pair of orthogonal functions termed the velocity potential  $\phi$  and stream function  $\psi$ . Both the velocity potential and the stream function are solutions of the Laplace equation with some specified boundary condition. In this way the Laplace equation relates the values of these functions in the interior of the computational domain to values at the boundary of the domain. If the stream function or the velocity potential is specified at all points on the boundary, then the stream function inside the boundary can be found and hence the complete flow field computed. This is convenient as in our problem the boundary condition at the free surface of the material is most easily phrased in terms of the velocity potential  $\phi$ , while the conditions at the other boundaries of the domain are most easily specified by the stream function  $\psi$ . For the purposes of the numerical model the boundary is specified at discrete points  $z_k$  as shown in Fig (2).

If suitable boundary conditions can be specified for the whole domain, then the complete flow field may be calculated. The only remaining problem is that of finding the position of the free surface. The position of the free surface is continually re-calculated by tracking the movements of points on the surface. The motion of these points is given by the most recently computed values of the flow field at these points.

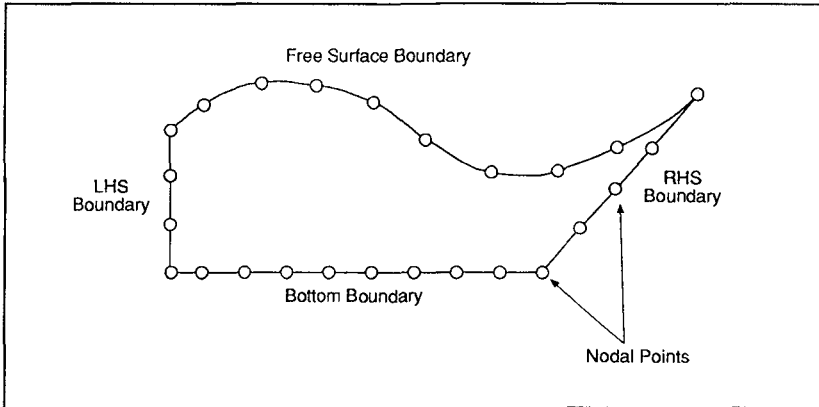


**Figure 2** The computational domain.

### 3.2 MATHEMATICAL FORMULATION

The orthogonal function defined by the velocity potential  $\phi$  and stream function  $\psi$  may be combined to form the complex potential;

$$\beta(z, t) = \phi(z, t) + i\psi(z, t) \quad (1)$$

In which  $z$  is a complex variable which describes the position in the computational domain;  $z = x + iy$  and  $t$  is the time variable.

As  $\phi$  and  $\psi$  both satisfy the Laplace equation,  $\beta$  must be an analytical function within the boundary of the fluid. For such an analytical function the value of  $\beta$  within the boundary can be related to the values of  $\beta$  at the boundary by use of the Cauchy integral theorem. If  $z_k$  is some point inside the boundary  $C$  then:

$$f(z_k) = \frac{1}{2\pi i} \oint_C \frac{f(z)}{z - z_k} dz \quad (2)$$

We are interested in the case when  $z_k$  also lies on the boundary. In this case if the boundary  $C$  is smooth, then  $z_k$  is related to all other points on the boundary by:

$$-i\pi\beta(z_k, t) + \oint_C \frac{\beta(z, t)}{z - z_k} dz = 0 \quad (3)$$

Equating the real and imaginary parts of Equ(3) produces two equations for the conditions where either  $\phi$  or  $\psi$  is known at the boundary point  $z_k$ :

$$\pi \psi(z_k, \hat{t}) + \operatorname{Re} \oint_C \frac{\beta(z, \hat{t})}{z - z_k} dz = 0 \quad (4)$$

for  $z_k$  lying on the boundary for which  $\phi$  is known

$$\pi \phi(z_k, \hat{t}) + \operatorname{Re} \oint_C i \frac{\beta(z, \hat{t})}{z - z_k} dz = 0 \quad (5)$$

for  $z_k$  lying on the boundary for which  $\psi$  is known

For purposes of the numerical calculation, the boundary is divided into discrete points. By assuming a linear variation of  $\beta$  between the points, the integral around the boundary can be expressed in terms of a summation over an influence function. The set of equations formed by this summation for each point is then assembled into a matrix. The matrix is solved by Gaussian elimination to produce  $\phi$  and  $\psi$  at each point on the boundary.

### 3.3 BOUNDARY CONDITIONS

There are four boundaries on which conditions must be specified.

**THE IMPERMEABLE BOTTOM BOUNDARY:** Here the condition is no flow normal to this boundary, which results in:

$$\psi = \text{constant}$$

In our case the constant = 0

**THE LEFT HAND BOUNDARY:** This boundary condition is supplied by the wave maker and the simple theory of wave generation proposed by Galvin (1964) is used. The wave maker is simulated as a piston that produces flow normal to this boundary, hence at this boundary  $\psi$  is specified. In addition to the original model developed by Shih, this boundary has been modified to allow wave energy to exit the computational domain.

**THE RIGHT HAND BOUNDARY:** This is the interface with the internal flow model. Flow normal to the boundary is given by the seepage flow from the internal model at this interface. Here  $\psi$  is again specified.

**THE FREE SURFACE BOUNDARY:** At this boundary two conditions are required, one to specify the velocity potential and another to describe how this boundary should move between time steps.

The velocity potential is given by the dynamic condition:

$$\frac{\partial \phi}{\partial t} = ww^* - gy - \frac{p_s}{\rho} \quad (6)$$

Where  $w = u - iv$  the conjugated complex velocity,  $g$  = acceleration due to

gravity,  $y$  = the vertical position of the boundary point,  $p_s$  = the pressure at the surface (in most cases  $p_s = 0$ ),  $\rho$  = density of the fluid

Hamming's fourth order predictor-corrector method is used to determine  $\phi$  from Equ(6) with the exception of the first three time steps of a calculation when the Runge-Kutta method is used.

The new position of the boundary is calculated from the kinematic condition:

$$\frac{Dz}{Dt} = \frac{D}{Dt}(x+iy) = w^* \quad (7)$$

Where  $z$  = the complex position of the boundary point (which has coordinates  $x$  and  $y$ ). This allows the new position  $z$  of the boundary to be calculated for the next time step by an integration over time  $t$ .

#### 4. THE INTERNAL FLOW FIELD

As in the external flow model the internal flow model is two-dimensional, with the breakwater cross section forming the computational domain. Wave motion is caused by the variation of the pressure on the seaward face of the structure and fluid flow through the structure. The front face of the breakwater forms the interface of the two models. The pressures on this external face are supplied by the external flow model.

##### 4.1 THE GENERAL PRINCIPLES

The problem is one of seepage flow through a porous granular medium, with a free surface within the medium. The granular material of the breakwater is of sufficient size that the flows within the medium are turbulent and may not be described by Darcy's linear law. The existence of an exact relationship between hydraulic gradient  $i$ , and the bulk flow velocity  $u$ , is in this case uncertain, however recent research by Williams, Burcharth, & den Adel (1992) indicates that the Forchheimer equation forms the best fit to the empirical data available at present. The unsteady flow form of the Forchheimer equation is:

$$i = au + bu^2 + \frac{(1+C)}{g} \frac{\partial u}{\partial t} \quad (8)$$

Where  $a$  and  $b$  are the Forchheimer coefficients which are dependent on the granular material. Separate layers of filter material within the breakwater result in  $a$  and  $b$  being functions of position.  $C$  is the virtual mass coefficient and is also dependent on the material. Means of determining values for  $a$ ,  $b$  and  $C$  are discussed in the paper by Williams et al. (1992).

The assumption that the fluid is incompressible provides the continuity equation in the form

$$\nabla u = 0 \quad (9)$$

The Forchheimer equation and the equation of continuity with adequate boundary conditions are sufficient to allow the flow field to be solved uniquely.

The flow field is calculated by use of a finite element method where the computational domain is defined by the breakwater cross section and the phreatic surface of the water. The phreatic surface rises and falls with the wave motion. As a result the size and shape of the computational domain is also a function of time. The position of the phreatic surface must therefore be calculated at each time step and the finite element mesh re-fashioned to fit the new computational domain.

## 4.2 MATHEMATICAL FORMULATION

It is useful to phrase the Forchheimer equation in terms of the piezometric head  $P_p$ .

$$-\nabla P_p = (a+b|\bar{u}|)\bar{u} + \frac{(1+c)}{g} \frac{\partial \bar{u}}{\partial t} \quad (10)$$

the piezometric head is related to the pressure  $p$  by:-

$$P_p = \frac{p}{\gamma} + y \quad (11)$$

where  $y$  is the some vertical coordinate.

The time domain is dealt with by the use of finite differences. Writing:

$$\frac{\partial \bar{u}}{\partial t} = \frac{(\bar{u}|_{t+\Delta t} - \bar{u}|_t)}{\Delta t} \quad (12)$$

Substituting Equ(12) into Equ(10) gives:

$$\bar{u}^{t+\Delta t} = K \left( \Delta(P_p)|_{t+\Delta t} - \frac{1+C}{g\Delta t} \bar{u}^t \right) \quad (13)$$

where

$$K = \frac{1}{a+b|\bar{u}| + \frac{(1+C)}{g\Delta t}} \quad (14)$$

is the conductivity of the rubble material. Note that  $K$  is a function of  $u$ .

Substituting Equ(14) into the continuity equation (Equ(9)) yields the governing equation for the piezometric head:

$$\Delta( K \Delta P_p ) = 0 \quad (15)$$

For the purposes of the numerical simulation this equation is re-phrased as the requirement that:

$$\chi = \iint_A K \left[ \left( \frac{\partial P_p}{\partial x} \right)^2 + \left( \frac{\partial P_p}{\partial y} \right)^2 \right] dx dy \quad (16)$$

should be a minimum for the given boundary conditions and the integration is carried out over the whole of the computational domain. Finite element discretization of this equation is carried out using triangular mesh elements. The minimisation technique produces a set or matrix of equations that can be solved to give the piezometric head and flow velocities for the specified boundary conditions.

### 4.3 BOUNDARY CONDITIONS

For the internal flow the boundary conditions are specified in terms of the piezometric head  $P_p$ . There are four relevant boundaries:

**THE BOTTOM BOUNDARY:** This boundary is impermeable so the condition of no flow normal to this boundary gives:

$$\frac{\partial P_p}{\partial y} = 0 \quad (17)$$

where  $y$  is the vertical coordinate.

**THE HARBOUR SIDE BOUNDARY:** At present, this boundary has been kept simple by specifying that the water level behind the breakwater remains constant at  $y=d$ . Hence:

$$P_p = d \quad (18)$$

**THE SEAWARD BOUNDARY:** This is the interface between the internal and external models. Here the boundary condition is supplied by the pressure distribution given by the external model.

$$P_p = \frac{\rho}{\gamma} + y \quad (19)$$

Continuity of flow through this boundary is achieved by the coupling technique described in the next section.



THE PHREATIC SURFACE BOUNDARY: Since this boundary moves, two boundary conditions are required.

The kinematic boundary condition:

$$\frac{Dx}{Dt} = u, \quad \frac{Dy}{Dt} = v \quad (20)$$

where  $x$  and  $y$  are the coordinates of the boundary point and  $u$  and  $v$  at the flow velocities at these points.

The dynamic boundary condition:

$$P_p = \gamma \quad (21)$$

At time  $t = 0$ , the initial conditions are:

$$P_p = \text{const.} \quad \bar{u} = 0 \quad (22)$$

## 5 COUPLING OF THE INTERNAL AND EXTERNAL FLOW MODELS

The external flow model is coupled to the internal flow model by demanding continuity of flow and pressures through the shared boundary. This is achieved by use of a trial and error technique as shown in the flow chart in Fig(3).

It is this coupling of the external and internal flow regimes that makes the completed model unique. This technique allows the wave motion onto and through the breakwater to be simulated without the need for additional data to be supplied from physical model tests.

## 6 PHYSICAL MODEL TESTS

Work carried out at Wallingford for the Single Layer Armour Unit Research Club has provided an excellent opportunity to obtain empirical data against which the numerical model can be tested. The study involved the construction of a model rubble mound which was armoured with model units.

The rubble mound was constructed with the geometry as shown in Fig (4). The core material was crushed limestone ranging in size from 4-6mm, the underlayer consisted of 10-14mm limestone. The armour units were simulated by a plastic frame work of the appropriate porosity or by model units of the correct density.. During construction care was taken to carefully weigh all the core and filter material used in the model so that the porosity of the relevant layers could be determined. These porosities must be known to allow the correct determination of the Forchheimer coefficients  $a$  and  $b$  used in the numerical model.

During the construction the pressure transducers were buried in the positions

shown. The cables of these transducers exited the rear of the mound and connected to the appropriate equipment to allow the pressures to be monitored by computer.

In order to make the comparison of the numerical simulation and the physical model test data as simple as possible, only data from regular wave conditions have been investigated. The wave conditions tested ranged in height from 0.11 to 0.2m and in period from 1.6 to 2.8s. The piezometric heads measured by the pressure transducers were logged by computer for each test condition.

The numerical model was run for a structure with the same geometry and material properties as the physical model. The values of the Forchheimer coefficients  $a$  and  $b$  were determined by comparison of the core and filter material with material whose permeability had previously been measured at HR, (see Williams et al. (1992)). The piezometric head at the positions of the pressure transducers was determined from the internal flow model and compared to the physical model data as described in the next section.

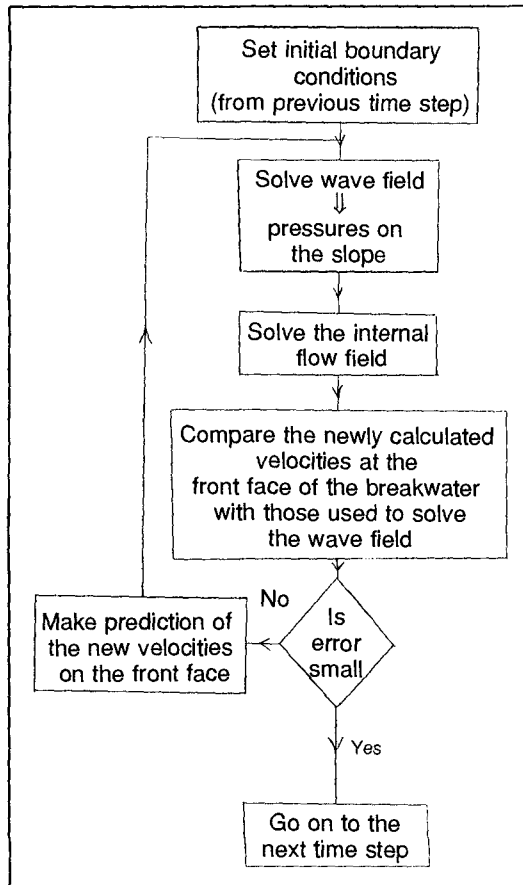


**Figure 3** Linkage of Wave and Internal Flow Models.

## 7 RESULTS

The flow of fluid within the mound is illustrated as a velocity plot in Fig. (5.a-d). The wave height is 0.14m with a period of 2.4s. It is seen that the majority of the fluid flow occurs within the armour and filter layers. This is expected as the armour and filter layers are several orders of magnitude more permeable than the core of the breakwater. Points on the phreatic surface are marked  $\circ$ .

In Fig.(6.a-e) show the predicted and observed pressures at the positions of

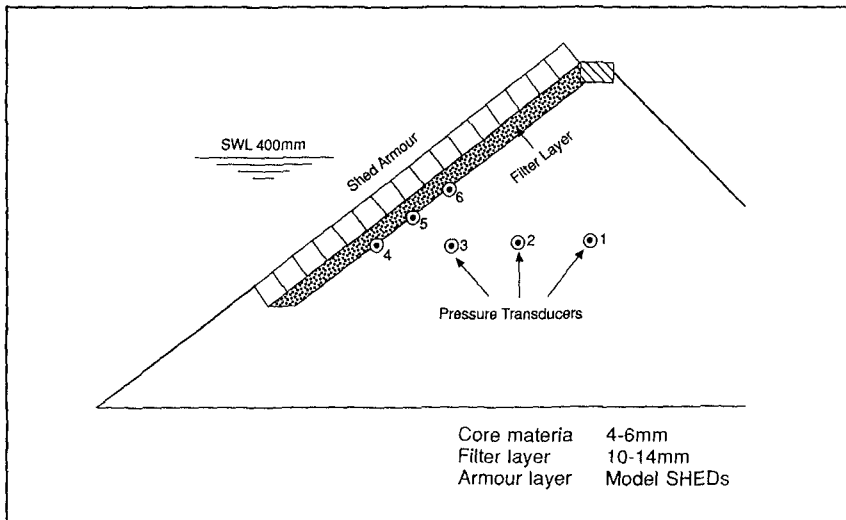


**Figure 4** Locations of the pressure transducers.

the pressure transducers within the mound. The close match between the empirical data and numerical results is very encouraging. The discrepancy between the observed and predicted pressures for positions deep within the mound is probably the result of the boundary condition, of constant water level behind the mound imposed on the internal flow model. Replacement of this boundary condition would allow wave motion behind the breakwater, and reduce the amount of predicted of wave attenuation within the mound. It may be possible to model the wave motion behind the breakwater, by applying the boundary element method to this region and demanding continuity of flow through the rear face of the breakwater as for the front face.

The discrepancies between observed and predicted pressures for high wave conditions may be the result of the effects of wave breaking that cannot be modelled with the boundary element technique described. The use of empirically derived correction factors might be of use in reducing this error, however this would require an extensive series of physical model tests. Such a series of tests would circumvent the advantages of this model over the internal flow model developed by Hannoura & McCorquodale (1985).

The model at present is sometimes unstable. Problems may be encountered in establishing continuity of flow across the external/internal interface with sufficient accuracy. This may be due to the fundamental differences in the models used to calculate the external and internal flows, and the assumptions that these models are based upon. The boundary element model used for the external flow requires the assumption that the flow is irrotational. No such restriction is placed on the internal finite element model. Such inconsistencies of formulation may well be the source of the observed inability to match the

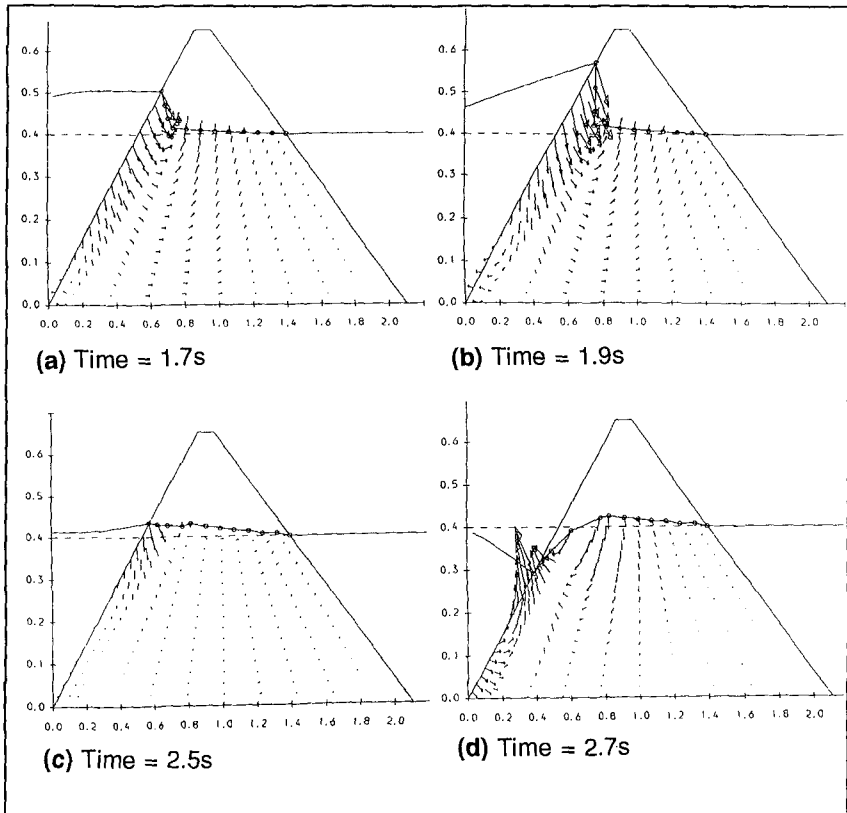


**Figure 5** Velocities within the mound

flow through the interface. The nature of the instability requires further study so that the conditions that lead to it may be predicted. Until this time the model must be used cautiously and the results interpreted with care.

## 8 CONCLUSIONS

There is a good agreement between predicted and observed pressures near the front face of the breakwater mound for waves of moderate height. The accuracy of the model declines when significant wave breaking and air entrainment occurs.

The model under predicts the amount of wave action deep within the mound. This is almost certainly due to the effects of an unrealistic boundary condition applied to the harbour side of the breakwater. Correction of this boundary condition should significantly improve this aspect of the model.

The full modelling of wave action that includes wave breaking and the

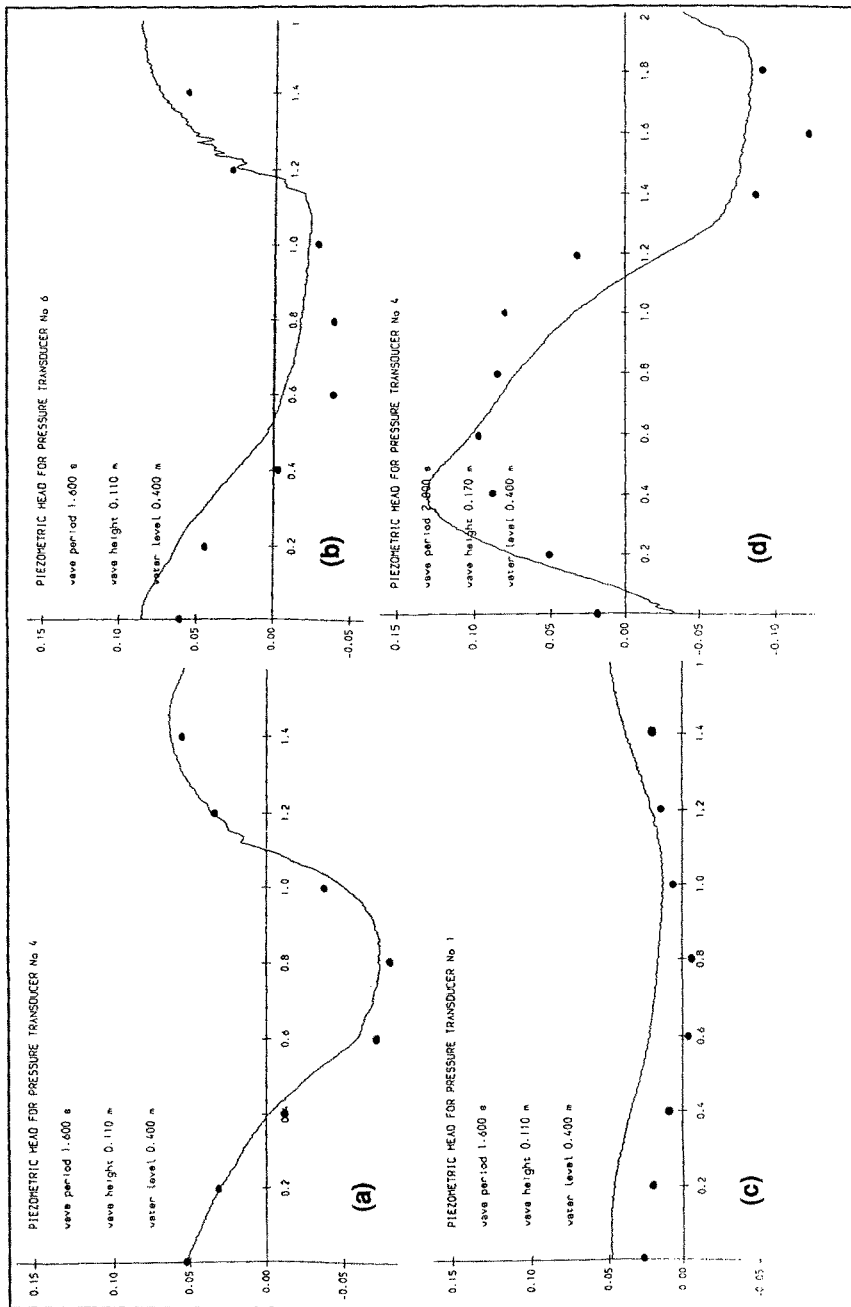


Figure 6 Predicted • and observed pressures within the mound.

entrainment of air must wait for the development of volume of fluid methods as described in the introduction. Until VOF models are available for implementation on small computers, composite models such as this will continue to provide valuable insight into the nature of flows within the cores of rubble mound breakwaters.

## 9 ACKNOWLEDGEMENTS

The collection of physical modelling data and the comparison of this data with the numerical model described in this paper was supported by Single Layer Armour Unit Research Club, co-funded by the Department of the Environment Construction Industry Directorate. Work on the development of the numerical model was funded by Dalian University Of Technology, the British Council and HR Wallingford. The presentation of this paper was supported by HR Wallingford.

## 10 REFERENCES

- Galvin,C.J. "Wave height prediction for wave generators in shallow water". Tech. Memo 4, U.S. Army, Coastal Engineering Research Centre, Mar. 1964.
- Hannoura,A.A. "Numerical and experimental modelling of unsteady flow in rockfill embankments". PhD Thesis, University of Windsor, Windsor, Canada, 1978.
- Hannoura,A.A. & McCorquodale,J.A. "Rubblemounds: numerical modelling of wave motion". Journal of Waterway, Port, Coastal and Ocean Engineering, Volume III, Number 5, September 1985. pp 800-816.
- Madsen,O.S. & White,S.M. "Wave transmission through trapezoidal breakwaters", Proc. 15<sup>th</sup> International Conf. on Coastal Engineering, 1976. Chap 153.
- McCorquodale,J.A. & Nasser,S.M. "Numerical methods for unsteady Non-Darcy flow". Proc. International Symposium on Finite Element Methods in Flow Problems, University of Wales, United Kingdom, January 1974. pp 545-551.
- van der Meer,J.W., Petit,H.A.H., van der Bosch,P., Klopman,G., & Broekends,R.D. "Numerical simulation of wave motion on and in coastal structures". Proc. 23<sup>rd</sup> International Conf. on Coastal Engineering, 1992.
- Nasser,M.S. "Theoretical and experimental analysis of wave action in rockfill structures". PhD Thesis, University of Windsor, Windsor, Canada, 1974.
- Nichols,B.D., Hirt,C.W., & Hotchkiss,R.S. "SOLVA-VOF: A solution algorithm for transient fluid flow with multiple free boundaries". Report LA-8355 Los Alamos Scientific Laboratory, Univ. of California. 1980.
- Shih,R.W.K. "Wave induced uplift pressures acting on a horizontal platform". PhD thesis, University of London, 1989.
- Sollitt,C.K., & Cross,R.H. "Wave transmission through permeable breakwaters", Proc. 13<sup>th</sup> International Conf. on Coastal Engineering, 1972. Chap 103.
- Vinje,T., & Brevig,P. "Numerical simulation of breaking waves". Advanced Water Resources 4, pp 77-82, 1981.
- Williams,A.F, Burcharth,H.F, & den Adel,H. "The permeability of rubble mound breakwaters. New measurements and new ideas". Proc. 23<sup>rd</sup> International Conf. on Coastal Engineering, 1992.